

Micro-Mechanical and Electrochemical Behaviour of Eco-Friendly Agro-Residue Composite Brake Pad Liner

M. O. Okunlola^{1*}, K. O. Abdulrahman¹ and A. S. Adekunle¹

¹*Department of Mechanical Engineering, University of Ilorin, Ilorin, Nigeria*

*Corresponding Author: okunlolanrewajumojeed@gmail.com

Received 15/07/2025; accepted 05/12/2025

<https://doi.org/10.4152/pea.2027450511>

Abstract

Brake pads in automobiles are crucial, since their effectiveness determines the safety of vehicles in operation. Alternatives for brake pad liners are continuously being researched as a way of replacing detrimental materials such as asbestos and graphite. This research was aimed at developing some eco-friendly brake pad liners with agro-residue materials. The brake pad liners were produced using compression moulding employing particle sizes of three different sieve ranges of 400-300, 300-250 and 400-00 μm . The composite materials for brake pad liners production included seashell, sawdust, palm kernel shell (PKS) and charcoal, serving the functions of structural, filler, abrasive and lubricant, respectively, while the binder used to hold the composite together was epoxy resin (polyepoxide) mixed with hardener (diethylenediamine) in 2:1 ratio. Microstructural analysis conducted on three samples, formulated based on selected sieve ranges, displayed the composite arrangement in the formulation, and the effect of particle sizes. Sample C (400-00 μm) displayed an evenly distributed and closely packed particle sample. Results revealed that hardness of the composite material decreased with smaller sieve ranges. Sample C, with the compressive strength of 4.0839 MPa, had lowest hardness value and highest thermal stability of 394 °C, with corrosion rate of 0.0056 mm/yr.

Keywords: automobile; brake pad; hardness; microstructure; structural material.

Introduction*

Braking systems in automobiles have the function of controlling the speed of a vehicle in motion by overcoming its momentum through an energy conversion mechanism induced through the wheel by friction between two surfaces (brake pad and rotor). This is achieved through energy conversion from kinetic to heat energy, thus reducing motion, and eventually bringing it to a rest position when engaging for a certain period of time [1-3]. The performance of a good brake pad is often determined by the effectiveness of its liner during the braking operation, when the brake is engaged in moving the vehicle. So, this liner should be made of a material with moderate frictional coefficient, good wear resistance, as compared to the rotor resistance, appropriate thermal stability, even distribution across the friction lining, and suitability of its usage under any weather condition [4-7]. All these parameters are dependent of the friction liner constituents, as a single material cannot

*The abbreviations list is in page 532.

displayed all required properties [1, 3], and of the distribution of the material forming the brake pad liner [8].

The braking operation could be achieved either: mechanically, as found mostly in parking car by restriction of its movement, even when it is on a slightly sloped terrain; hydraulically, when hydraulic fluid is used as a means of transferring the pressure from the brake pedal to the pad; or pneumatically, which is majorly employed in commercial vehicles where higher braking efficiency is required due to the higher momentum to be overcome [9]. For all these modes of power transmission from the brake pedal to the receiving end (brake pad), wear usually builds up due to friction between surfaces in contact (i.e. brake pad and disc) [10, 11]. Thus, proper monitoring should be conducted and replacement be made on a regular interval, either with distance coverage method or based on usage duration [1].

There are different classes of friction materials that are employed, but asbestos-lined type of brake pad was mostly used due to its outstanding performances and characteristics, including low density, moderate mechanical properties, good thermal resistance, appropriate frictional coefficient and excellent wear resistance to disc [3]. Brake friction liner usually contains four major important constituents which are binders, fillers, lubricant/frictional modifiers and reinforcement, in which asbestos has been majorly used as filler with phenolic resin, graphite and silica oxide/steel dust as binder, lubricant and reinforcement/abrasive, respectively [13]. However, researches have deemed asbestos carcinogenic to human respiratory organs, which has led to its usage ban for brake pad production in over sixty countries of the world [1, 12], after its trace to diseases known as asbestosis, mesothelioma, lung cancer and others has been confirmed. This has led researchers to investigate for potential and permanent materials in automobile industry that have similar properties or better performance compared to asbestos-lined brake pads [1, 14, 16, 18]. Thus, the use of industrial and agricultural waste, such as seashell, sawdust, palm kernel shell (PKS) and charcoal, as base material, fillers, abrasive and friction modifier/lubricant, respectively, and epoxy resin, as binding agent for brake friction liner, can be of economic value, means of foreign exchange and environmental beneficial for the country [1, 16, 19]. Also, eco-friendly agro-animal residues, such as palm fruit fibre, bush mango nutshell, coconut, egg, periwinkle, snail, cocoa beans and shea nut shells, cow bones, hooves and horns, rice husk, bamboo leaves, sawdust, maize husk, banana peels and bagasse, have displayed a huge potential for brake pad application [16, 20-22, 30].

Therefore, this research examined micro-mechanical and electrochemical behaviour of brake pad liners made from composites of eco-friendly agro-residues material, alongside other environmental friendly additives, with the aim of total replacing asbestos and other synthetic additive material constituents in brake pads. The reference brake pad purchased from market is presented in Fig. 1.



Figure 1: Reference commercial brake pad sample.

Methodology

Material sourcing and collection

The materials used for this research were seashell, sawdust, PKS, charcoal, epoxy resin (polyepoxide) and hardener (diethylenediamine). Clam seashell (*Mercenaria mercenaria*) was adopted due to its excellent structural and thermal stability properties, and readily availability, and it was collected at Ajah beach, Lagos state. Ayunre (*Albizia zygia*) sawdust and white kola charcoal (*Garciana cola*), of trees with approx. 8 and 10 years of age, respectively, were collected at Igbo-alahun village, Oyo State. PKS (*Elaeis guinensis*) was sourced and collected at Iyeku Osun State. Epoxy resin (Polyepoxide) and hardener (Diethylenediamine) were used for their excellent properties, such as wear and crack resistance and higher structural stability at elevated temperatures, and were purchased at Ojota chemical market (Lagos).

Material preparation

Raw materials (seashell, sawdust, PKS and charcoal) were dried under sun for seven days, with average time of 5 h per day, to remove surface moisture. They were grinded with attrition milling, and sieved using three different sieve ranges of 400-300, 300-250 and 400-00 μm . Epoxy resin (Polyepoxide) and hardener (Diethylenediamine) were mixed in ratio 2 to 1, as shown in Fig. 2, which is in agreement with the formulation of brake pad liner produced from sawdust composite [31].

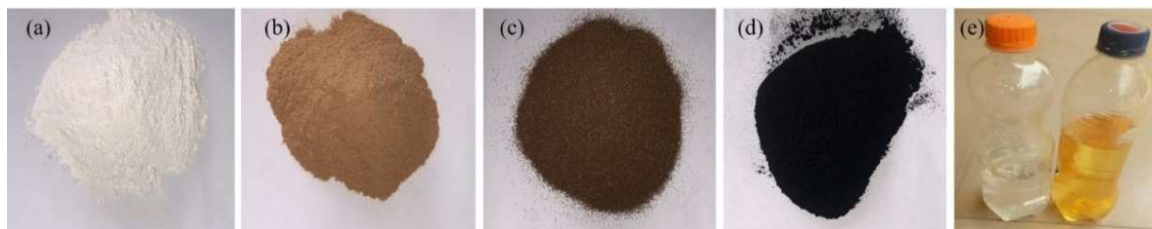


Figure 2: (a) seashell, (b) sawdust (c), PKS and (d) charcoal as pulverized materials; (e) epoxy resin and hardener.

Sample formulation and production

Composite formulations were prepared using three different particle sizes of seashell, sawdust, PKS, charcoal and binder contents, as shown in Table 1, based on the modification suggestion [1].

Table 1: Sample formulation for production.

Composite	Sieve ranges (μm)	Seashell	Sawdust	PKS	Charcoal	Binder	Total
Sample A	400 - 300	30	20	17	6	27	100
Sample B	300 - 250	30	20	17	6	27	100
Sample C	400 - 0	30	20	17	6	27	100

Selected materials – 30 g seashell, 20 g sawdust, 17 g PKS and 6 g charcoal – were thoroughly mixed with an electric-powered mechanical mixer, for ten min, to give a homogeneous material mixture. Epoxy resin and hardener, with ratio 2:1, were mixed in a separate container. Production flowchart is presented in Fig. 3.



Figure 3: Brake pad liner production flowchart.

The two mixtures were then blended with a mechanical mixer, until a low-moisture homogenous mixture was formed. Then, the blended mixture was compressed in a fabricated metallic mould of 1400 mm³ volume and placed on a backing plate (cut into dimensions to be accommodated by the brake calliper) of 4 mm thickness (high carbon steel plate). Compressive force of 40 kN was applied to bind the material with the backing plate, for 5 min holding time, under the compression testing machine (STYE-2000) shown in Fig. 4.

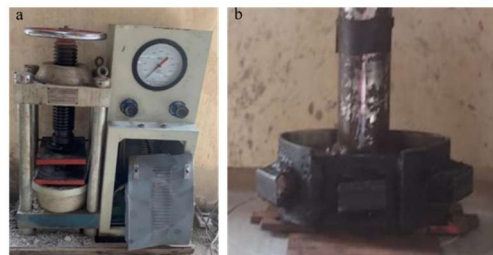


Figure 4: (a) Compression testing machine and (b) mould and die.

Afterwards, the brake pad was ejected from the mould, and kept at room temperature, for 24 h, before being cured in an electric oven, at 150 °C, for 60 min. Fig. 5 shows the produced brake pad.



Figure 5: Produced brake pad samples.

Micro-mechanical and electrochemical behaviour of brake pad liners

The following experiments were carried out on the brake pad liner to determine its microstructural, hardness and corrosion behaviour for better comparing the samples' performances.

Hardness test

Hardness test was conducted using Monsanto Testing Machine for hardness and shearing (Fig. 6), to determine Brinell hardness of the samples (BHN).



Figure 6: Monsanto testing machine for hardness and shearing.

Samples were cut to a specific square shape of 30 by 30 mm and thickness of 12 mm. Then, they were fixed into the tensiometer, to be subjected to compression of load of 1250 kg, for 20 sec., after which the indented diameter was measured by eye scope. BHN, which is the pressure per unit surface area of identification in kg per square meter, was calculated using Eq. (1):

$$\text{BHN} = \frac{W}{\left(\frac{\pi D}{2}\right) \times (D - \sqrt{D^2 - d^2})} \quad (1)$$

where W is load on indenter (kg), D is diameter of steel ball (mm) and d is average measured diameter of indentation (mm).

Compressive strength test

Compression test on the samples was conducted using universal testing machine (Model: INSTRON 3369), as shown in Fig. 7.



Figure 7: Universal Testing Machine.

Compression of the brake pad liner was investigated by placing the sample between the compression plates provided in the adjustable and bottom crossheads. The sample was properly positioned and gripped firmly between the compression plates, while load was gradually applied on it, and corresponding compressive strain was recorded at regular intervals. The process was repeated for the other samples. [32-34].

Thermogravimetric analysis

Thermogravimetric analysis was conducted on the samples using TGA 1000 model, for determining their thermal stability as temperature increased. It is generally known that the material's stability and performance varies with temperature increment, and failure occurs when thermal capability of the material is reached. Thus, different samples exhibit different thermal stability. The apparatus, which measures change in the sample's weight as temperature changes, is equipped with a furnace, a highly sensitive weighing meter located above the furnace, being thermally isolated from heat (Fig. 8).



Figure 8: Thermogravimetric analyser.

Corrosion test

Corrosion test was conducted using Gamry potentiostat/galvanostat/ZRA Reference 600+, based on ASTM G31 standard procedure. Corrosion testing is an inevitable step in material selection to establish the suitability of material for their intended use. It determines the resistance of materials to corrosion under certain environmental conditions, including temperature, humidity and exposure to chemicals.

Potentiodynamic polarization curves was performed in a conventional three electrodes cell using computer-controlled potentiostat/galvanostat (Gamry 600+). Platinum, Ag/AgCl, in 3 M KCl, and steel (with an exposure area of 10 mm²) were used as counter, reference and working electrodes, respectively. The electrodes were allowed to corrode freely for two h (120 min). After this procedure, a steady-state open circuit potential corresponding to corrosion potential of the working electrode was obtained. The procedure was repeated for each sample, with a fresh solution of 3.5% NaCl, to simulate sea water corrosion, at the scan rate of 5 mV/s. Fig. 9 shows the picture of corrosion test instrument.

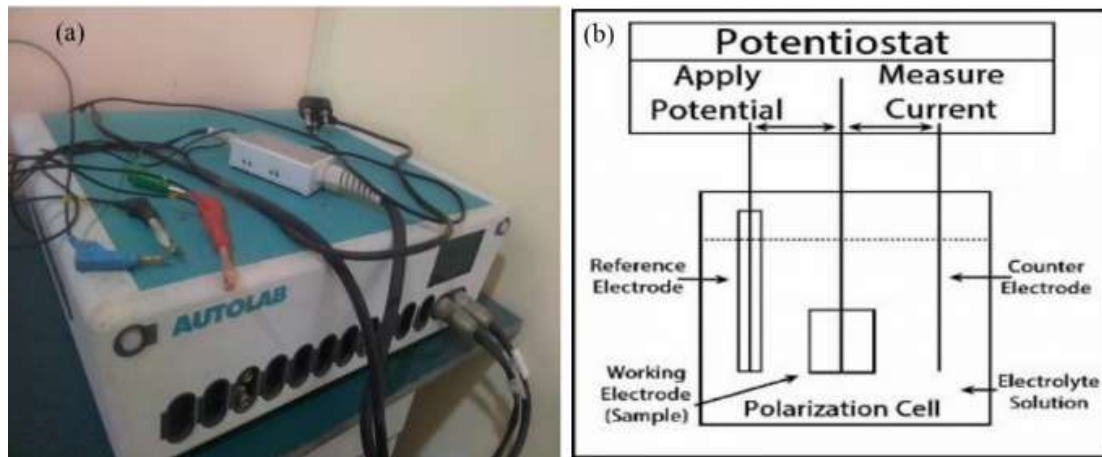


Figure 9: (a) Gamry potentiostat; (b) schematic picture of corrosion instrument.

SEM-EDS

This non-destructive micro-chemical analysis (SEM-EDS) provides chemical analysis of the field of view or spot analysis of minute particles, with high-resolution detailed image of the sample, by a focussed electron beam across its surface, detecting its secondary or backscattered electron signal (Fig. 10).



Figure 10: SEM-EDS analyser.

Results and discussion

Hardness assessment

Fig. 11 shows hardness behaviour of the composite with respect to the control sample. It was established that the hardness of the material decreased uniformly with reduced sieve ranges from 400–300 μm , in sample A, to 300–250 μm , in sample B. Closeness of hardness value of sample C (400-0 μm) is attributed to the interwoven of different grade of particle sizes forming a highly closed packed composite, which resulted in higher density of the formulated sample. Hardness value of control brake pad lining material was 153.95 BHN. Sample A, with 153.51 BHN, had the highest hardness value among the produced samples. Sample C had the lowest hardness of 123.21 BHN. This behaviour is known as inverse Hall-Petch effect [35,] due to the crystalline structure of the base material (seashell).

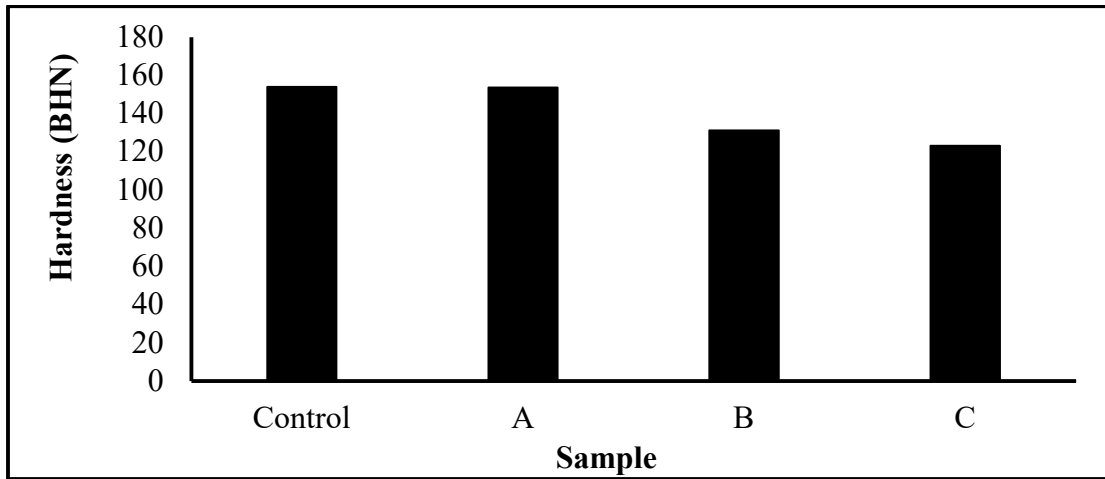


Figure 11: Comparison of hardness of produced samples with the control friction sample.

Compressive assessment

Fig. 12 demonstrates that compressive stress, energy at break and compressive extension at break of the composite friction materials increases from sample A to C. This shows that the brittleness of the produced friction materials decreases with increased particle sizes, which resulted in higher energy requirements to break the specimen. Higher compressive extension at break of sample C was due to proper and homogeneous arrangement of particles in the sample. Compressive stress, extension and energy at break of sample C were 4.0839 MPa, 3.8996 mm and 4.0528 J, respectively, while those of conventional friction material were 13.8371 MPa, 2.2293 mm and 5.4460 J, respectively.

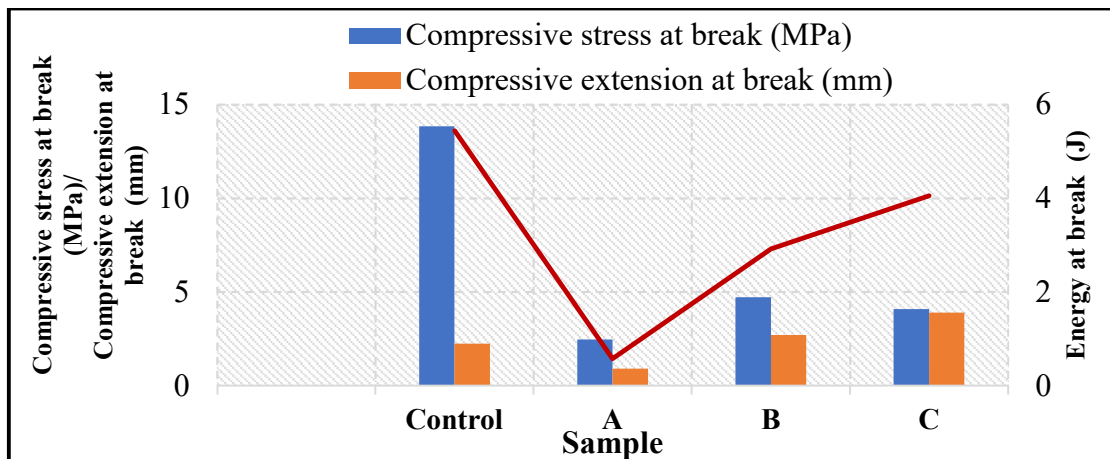


Figure 12: Compressive strength of produced samples with a control friction material.

Thermogravimetric analysis result

It could be generalized from Fig. 13 that the profile of the thermal behaviour degraded down step-wisely with an initial oxidation resulted in about 8% mass loss below 220 °C, which is associated with the formation of volatile matter during firing by the furnace.

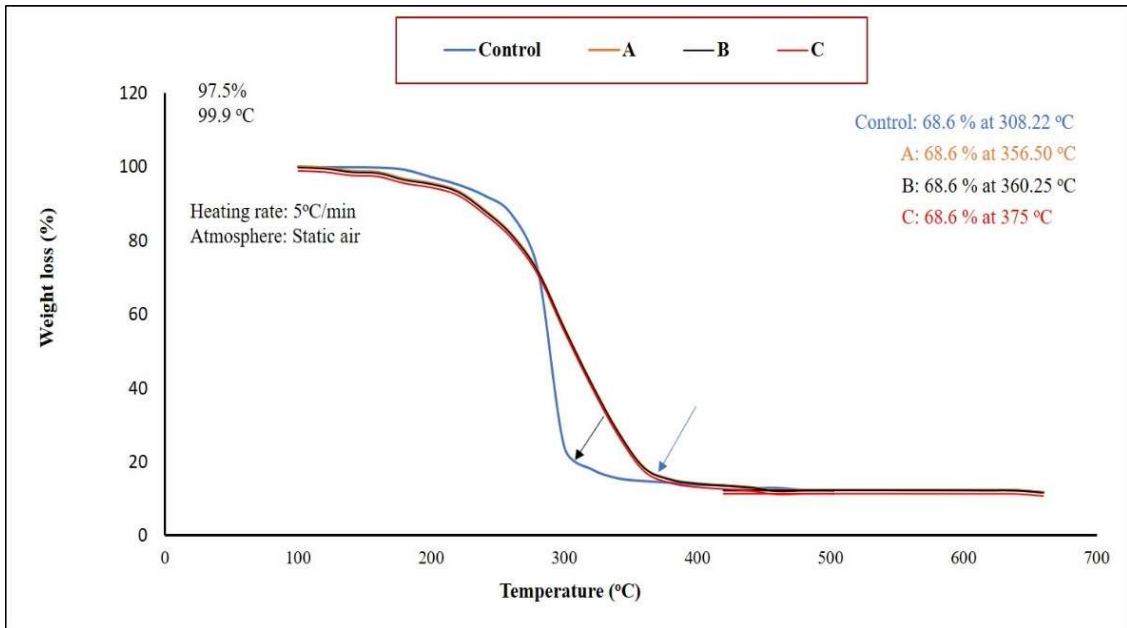


Figure 13: Comparison of thermal conductivity of produced samples with a control friction material.

Continuous heating to a temperature above 300 °C resulted in carbon oxidation of which produced samples showed a better stability to degradation in an oxidizing environment compared to reference commercial brake pad liner.

From the graph, control sample total weight loss at a temperature of 308.22 °C was 68.6%, which implies that there was a possible failure of the materials at approx. 300 °C.

The same amount of weight loss was at 356.50, 378.25 and 394 °C for the run of samples A, B and C formulated composite brake pad liners, respectively. In summary, the newly formulated brake pad liner (sample C) performed much better than the control sample at higher temperature, due to its high thermal stability which was 22.79% higher compared to the reference commercial sample. A similar trend was observed by [36].

SEM-EDS

Fig. 14 shows the arrangement of particle composition in the control friction material and in the produced samples.

The particles arrangement in the sample C composite friction material shows uniform distribution and closely packed arrangement in their sizes which resulted in an increase in density and corresponding stronger wear rate.

Higher hardness value of control sample is attributed to the closely packed particle of its content, which resulted in its brittleness due to the rise in compressive strength. The presence of elements like Ti, Si, and exposure to high Cl content, in the control sample have adverse effects on human health.

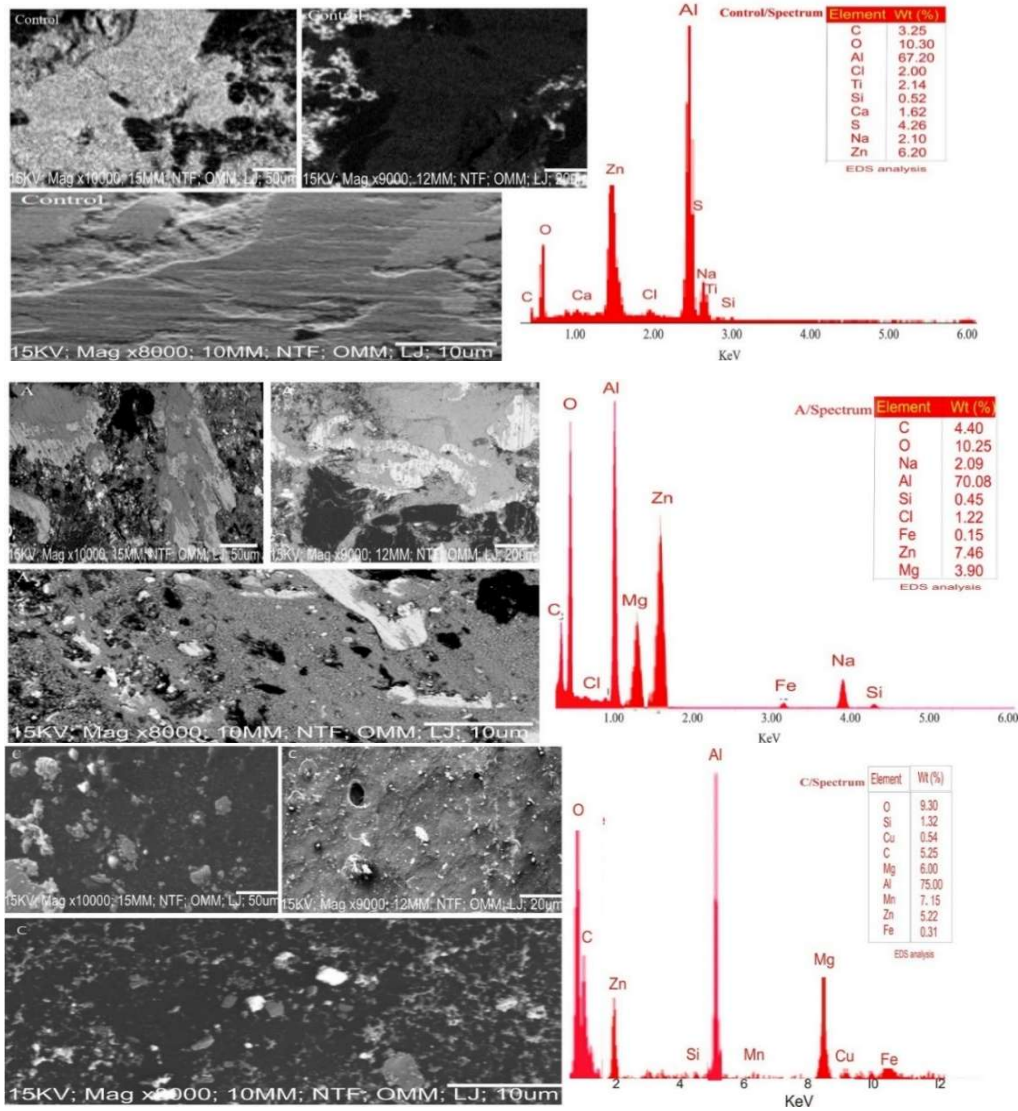


Figure 14: SEM/EDS results.

Corrosion test result

The result of corrosion test carried out is presented in Fig. 15.

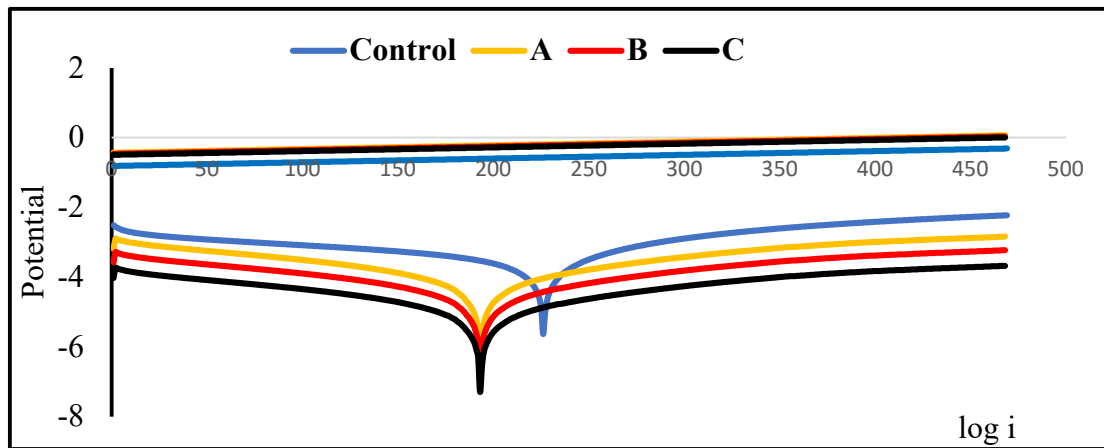


Figure 15: Comparison of corrosion rate of the control and produced samples.

According to the obtained value, it was revealed that the newly formulated brake pad material has a very high resistance to corrosion compare to the reference control sample. Corrosion rate of the three formulated composite material ranged from 0.0066, 0.0060 and 0.0056 mm/yr. for samples A, B and C, respectively, compared to its reference commercial sample with 1.4373 mm/yr., as shown in Table 2.

Table 2: Corrosion result data.

3.5% NaCl	E_{corr} (V)	j_{corr} (A/cm ²)	Corrosion rate (mm/yr)	Polaris. resist. (Ω)	β_a (V/dec)	β_c (V/dec)
Control	-0.5718	1.24E-04	1.4373	128.26	0.0587	0.0968
Sample A	-0.3425	3.85E-06	0.0066	2795.7	0.0736	0.0951
Sample B	-0.3022	4.23E-06	0.0060	2957.4	0.0784	0.0876
Sample C	-0.2876	4.81E-06	0.0056	3410.8	0.0810	0.0707

This result disclosed that the formulated composite material is extremely resistant to corrosion, and the usage of the material in the wet/moist environment has little or no effect on the performance of the brake pad liners when stored or packed on the vehicle for a long duration.

The control sample has a very high corrosive ability due to the present of metallic elements in the sample like Ti, and high percentage of S which reacted with other metals content like Mg, Al, Fe and Zn on the control sample to liberate hydrogen gas, which has caused its corrosivity [37].

Conclusions

Micro-mechanical properties of the formulated brake pad liners displayed an outstanding performance as compared to the reference commercial sample which accord its suitability as substitute for asbestos and other harmful additives in these materials. Particle arrangement of constituents of the developed brake pad liner revealed an evenly distributed constituents with no harmful elements presents. Hardness and corrosion rate of the produced liner reduced from sample A to C as the particle sizes decreases with hardness values of 153.51, 131.12 and 123.12 BHN and corrosion rate of 0.0066, 0.0060 and 0.0056 mm/yr. for samples A, B and C, respectively. Compressive strength increased with decrease in particle sizes of the formulated constituents with values of 2.4603, 4.7155 and 4.0839 MPa, for sample A, B and C, respectively, while hardness, compressive strength and corrosion rate of the control sample were 153.95 BHN, 13.8371 MPa and 1.4373 mm/yr.

Authors' contributions

M. O. Okunlola: conceptualization; investigation; wrote the original draft. **K. O. Abdulrahan:** conceptualization; reviewed and edited the manuscript. **A. S. Adekunle:** conceptualization; reviewed the manuscript.

Abbreviations

- BHN:** Brinell hardness number
EDS: Energy-dispersive X-ray spectroscopy
PKS: palm kernel shell
SEM: Scanning Electron Microscopy

References

1. Adekunle AS, Okunlola MO, Omoniyi PO et al. Development and analysis of friction material for eco-friendly brake pad using seashell composite. *International journal of science and technology. Sci Iran B.* 2023;5(30):1562-71. <http://doi.org/10.24200/SCI2022.59835.6464>
2. Kumar S, Priyadarshan K, Gosh KS. Comparative study of airborne particles on new developed metal matrix composite and commercial brake pad materials with ANN and finite element analysis, springer, compositional particle mechanism. *Lubric Sci.* 2023;35(6):1-1. <http://doi.org/10.1007/s40571-022-00491-9>
3. Popoola OT, Rabiun AB, Ibrahim HK et al. Production of Automobile Brake Pads from Palm Kernel Shell, Coconut Shell, Seashell and Cow Bone. *Adel Univ J Eng Technol.* 2021;4(2):2714-50.
4. Akıncioğlu G, Akıncioğlu S, Öktem H et al. Brake Pad Performance Characteristic Assessment Methods, *International Journal of Automotive Science and Technology. Int J Automot Sci Technol.* 2021;5(1):67-78. <http://doi.org/10.30939/ijastech.848266>
5. Harshvardhan Z, Ghetiya ND, Dipali P. Development of friction pad and study of its wear Characteristics. *Intern J Mech Prod Eng.* 2017;5(2):2320-92.
6. Crăciun AL, Pinca-Bretotean C, Birtok-Băneasă C et al. Composites materials for friction and braking application. *IOP Conf. Series: Materials Science and Engineering. Mater Sci Eng C.* 2016. <http://doi.org/10.1088/1757-899X/200/1/012009>
7. Ahmet A, Mukadder Y. Research on Wear Rate and Mechanical Properties of Brake Sabots (Shoes) Used in Railway Rolling Stocks. *Intern J Appl Sci Technol.* 2014;4(7):76-84.
8. Banait AS, Raibhole VN. Study on tribological investigation of alternative automotive brake pad materials. *IOSR J Eng.* 2019:40-43.
9. Oliyadi DF. Experimental and investigation of brake pad friction material with Corresponding Brake Disc for Toyota Hiace 5L Minibuses that used in Ethiopia City taxi. *Intern J Eng Innov Technol.* 2018;8(3):25-9.
10. Fadhel AA, Nader MM, Ehsan SA. Calculation of Wear Rate by Weight and Volume for Aluminum Samples. *Journal of University of Babylon for Engineering Sciences. J Univ Bab Eng Sci.* 2018;26(7):331-39.
11. Abdul HMK, Shasudin NI, Mat Lazim AR et al. Effect of Brake Pad Design on Friction and Wear with Hard Particle Present. *J Technol.* 2014;71(2):135-38. <http://doi.org/10.11113/jt.v71.3733>

12. Asonye U, Ofoma A, Duuanyim I et al. Development of automobile brake pad using three biological materials. *Nig J Eng Sci Res.* 2025;8(1):101-11. <https://doi.org/10.5281/zenodo.15829213>
13. Dineshkumar R, Ramanamurthy EVV, Krishnapavanteja Ch. Development of friction material by using precast prefired (pcp f) blocks. *Frontiers in Automobile and Mechanical Engineering. FAME. IOP Conf. Series: Mater Sci Eng.* 2017. <http://doi.org/10.1088/1757-899X/197/1/012001>
14. Ilori OO, Soji-Adekunle AR, Adedokun OP et al. Production of Automobile Brake Pads from Bagasse, Banana Peels and Periwinkle Shell. *Adel Univ J Eng Technol.* 2021;4(2):1-5.
15. Olele PC, Nkwocha AC, Ekeke IC et al. Assessment of Palm Kernel Shell as Friction Material for Brake Pad Production. *Intern J Eng Manag Res.* 2016;6(1):281-84.
16. Haruna VS. Evaluation of Sheanut Shell-Reinforced Automotive brake pad. *Arid Zone J Eng Techno Envir. Arid Zone J Eng Environ.* 2019;15(3):510-18.
17. Umamaheswara RR, Babji G. A Review Paper on Alternate Materials for Asbestos Brake Pads and Its Characteristics. *Intern Res J Eng Technol.* 2015;2(2):556-62.
18. Maleque MA, Atiqah A, Talib RJ et al. New Natural Fibre Reinforced Aluminium Composite for Automotive Brake Pad. *International Journal of Mechanical and Materials Engineering. Int J Mech Mater Sci.* 2012;7(2):166-70.
19. Yuvarag L, Jeyanthi S. An Investigation on Chemical Treatment of Phenol Formaldehyde with Natural Fibres for Brake Pads. *National Conference on Recent Trends and Developments in Sustainable Green Technologies. J Chem Pharm Sci.* 2015;7:419-21.
20. Onyenanu IU, Ofili I, Owuama KC. Eco-Friendly brake pad formulation using Agro-waste Derived Fillers: Bush Mango Nutshell and Palm Fruit Fibre Reinforced Composites. *Intern J Appl Nat Sci.* 2024;2(2):27-39. <http://doi.org/10.61424/ijans.v2.i2.152>
21. Gai PF, Adisa AB, Tokan A et al. A Review of Non-Asbestos Brake Pad Materials and the Future Trend. *Intern J Pure Appl Sci.* 2021;17(9):188-203.
22. Adekunle NO, Oladejo KA, Kuye SI et al. Development of Asbestos-free Brake Pads Using Bamboo Leaves. *Nig J Envir Sci Technol.* 2019;3(2):342-51. <https://doi.org/10.36263/nijest.2019.02.0126>
23. Uzochukwu MI, Aiyejagbara MO, Ugbaja MI. Property Investigation of Cowhorn/Periwinkle Shell Epoxy Composite for Automobile Brake Pad Linings. *J Emerg Trends Eng Appl Sci.* 2019;10(2):48-53.
24. Bello SA, Agunsoye JO, Adebisi JA et al. Physical Properties of Coconut Shell Nanoparticles. *J Sci Eng Technol.* 2016;12(1):63-79. <https://doi.org/10.3126/kuset.v12i1.21566>
25. Ikpabese KK, Gundu DT, Tuleun LT. Evaluation of Palm Kernel Fibre (PKF) for Production of Asbestos-free Automotive Brake pads. *J King Saud Univ Eng Sci.* 2014;1(20):110-18. <https://doi.org/10.1016/jksues.2014.02.001>

26. Onyeneke FN, Anaele JU, Ugwuegbu CC. Production of Motor Vehicle Brake Pad Using Local Materials (Periwinkle and Coconut Shell). *Int J Eng Sci.* 2014;3(9):17-24.
27. Amaren SG, Yawas DS, Aku SY. Effect of periwinkles shell particle size on the wear behaviour of asbestos free brake pad. *Res Phys.* 2013;3:109-14. <https://doi.org/10.1016/j.rinp.2013.06.004>
28. Ibhadode AOA, Dagwa I. Development of Asbestos-Free friction lining material from Palm kernel shell. *J Braz Soc Mech Sci Eng.* 2008;30(2):166-73. <https://doi.org/10.1590/S1678-58782008000200010>
29. Dagwa IM, Ibhadode AOA. Determination of Optimum Manufacturing Conditions for Asbestos-free Brake Pad Using Taguchi Method. *Nig J Eng Res Devel.* 2006;5(4):1-8.
30. Dagwa IM, Ibhadode AOA. Design and Manufacture of Automobile Disk Brake Pad Test Rig. *Nig J Eng Res Devel.* 2005;4(3):15-24.
31. Lawal SS, Bala KC, Alegbede AT. Development and production of brake pad from sawdust composite. *Leon J Sci.* 2017;30:1583-0233.
32. Ademoh AN, Adeyemi IO. Development and Evaluation of Maize Husks (Asbestos-Free) Based Brake Pad. *Industr Eng Lett.* 2015;5(2):67-80.
33. Adeyemi IO, Ademoh NA, Okwu MO. Development and Assessment of Composite Brake Pad Using Pulverized Cocoa Beans Shells Filler. *Intern J Materi Sci Applic.* 2016;5(2):66:78. <https://doi.org/10.11648/j.ijmsa.20160502.16>
34. Adeyemi IO, Ademoh NA, Thankgod EB. Development of Asbestos-Free Automotive Brake Pad Using Ternary Agro-Waste Fillers. *J Multidiscip Eng. Sci Technol.* 2016;3(7):5307-23.
35. Naik SN, Walley SM. The Hall-Petch and inverse Hall-Petch relations and hardness of nanocrystalline metals. *J Mater Sci.* 2020;55:2661-81. <https://doi.org/10.1007/s10853-019-04160-w>
36. Seth SA, Kankani CM. Production of brake pad material for industrial application. *Intern J Res Innov Appl Sci.* 2025;10(5):386-98. <https://doi.org/10.51584/IJRIAS>
37. Candan S, Unal M, Koc E et al. Effects of Titanium addition on Mechanical and Corrosion behaviours of AZ91 Magnesium alloy. *J All Comp.* 2011;50(9):1958-63 <https://doi.org/10.1016/j.jallc0m.2010.10.100>